

Substituted 1,3-Bis(imino)isoindole Diols: A New Class of Proton Transfer Dyes

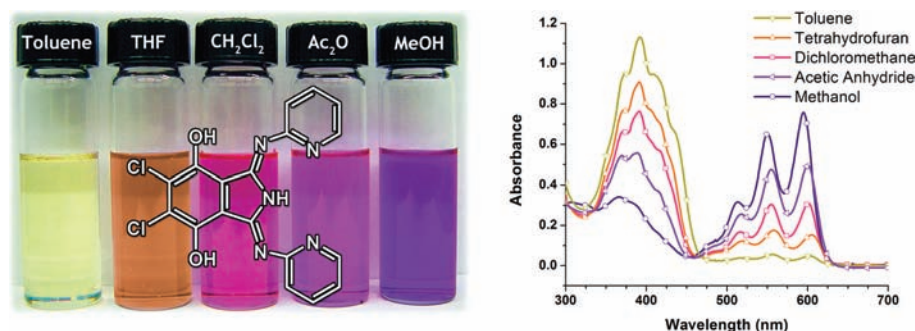
Kenneth Hanson, Niral Patel, Matthew T. Whited, Peter I. Djurovich, and
Mark E. Thompson*

Department of Chemistry, University of Southern California, Los Angeles, California
90089, United States

met@usc.edu

Received December 22, 2010

ABSTRACT



A new class of excited-state intramolecular proton transfer (ESIPT) dyes based on a 1,3-bis(imino)isoindole diol motif has been prepared. These molecules exhibit orange emission (~ 600 nm) with a large apparent Stokes shift (>6000 cm^{-1}) and quantum efficiencies up to 45%. Selective modification of the substituents can be used to shift the equilibrium between the enol and keto forms of the molecule in both the ground and excited states.

Molecules that undergo excited-state intramolecular proton transfer (ESIPT) are interesting for their distinct photophysical properties as well as their potential application as laser dyes,¹ fluorescent probes,² photostabilizers,³ high energy radiation detectors,⁴ and white-light emitting single molecules.⁵ In a typical ESIPT process, photoexcitation leads to a shift in electron density that facilitates proton migration from a donor atom, usually oxygen, to a nearby acceptor atom, often either oxygen or nitrogen. In

molecules with an oxygen donor, the ground state is described as the enol form, with hydrogen covalently bound to oxygen, and the emissive excited-state keto form, with hydrogen not covalently bound to oxygen. A large apparent Stokes shift is observed in luminescence due to the difference in energy between absorption by the original (enol) tautomer and emission from the resultant (keto) tautomer of the molecule.⁶ Recently, during our investigation of the photophysics of 1,3-bis(2-pyridylimino)isoindoline (**BPI**) derivatives⁷ we have found a new class of ESIPT dyes based on dihydroxyl substituted **BPI** compounds. Several derivatives are strongly emissive, and the position of the enol–keto equilibrium can be controlled by synthetic modification of the 1,3-bis(imino)isoindole diol structure.

The 1,3-bis(imino)isoindoline derivatives **1–7** (Table 1) were prepared in low to moderate yields using the method developed by Siegl,⁸ an alkaline-earth-catalyzed nucleophilic

(1) (a) Chou, P.; McMorro, D.; Aartsma, T. J.; Kasha, M. *J. Phys. Chem.* **1984**, *88*. (b) Acuña, A. U.; Amat-Guerri, F.; Costela, A.; Douhal, A.; Figuera, J. M.; Florido, F.; Sastre, R. *Chem. Phys. Lett.* **1991**, *187*, 98.

(2) (a) Sytnik, A.; Del Valle, J. C. *J. Phys. Chem.* **1995**, *99*, 13028. (b) Dennison, S. M.; Gubaray, J.; Sengupta, P. K. *Spectrochim. Acta, Part A* **1999**, *55*, 1127. (c) Holler, M. G.; Campo, L. F.; Brandelli, A.; Stefani, V. *J. Photochem. Photobiol. A: Chem.* **2002**, *149*, 217. (d) Shynkar, V. V.; Klymchenko, A. S.; Kunzelmann, C.; Duportail, G.; Muller, C. D.; Demchenko, A. P.; Freyssinet, J.-M.; Mly, Y. *J. Am. Chem. Soc.* **2007**, *129*, 2187.

(3) Chou, P.-T.; Martinez, M. L. *Radiat. Phys. Chem.* **1993**, *41*, 373. (4) Stein, M.; Keck, J.; Waiblinger, F.; Fluegge, A. P.; Kramer, H. E. A.; Hartschuh, A.; Port, H.; Leppard, D.; Rytz, G. *J. Phys. Chem. A* **2002**, *106*, 2055.

(5) Park, S.; Kwon, J. E.; Kim, S. H.; Seo, J.; Chung, K.; Park, S.; Jang, D.; Medina, B. M.; Gierschner, J.; Park, S. Y. *J. Am. Chem. Soc.* **2009**, *131*, 14043.

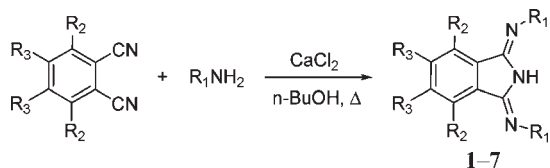
(6) Stephan, J. S.; Rodriguez, C. R.; Grellmann, K. H.; Zachariasse, K. A. *Chem. Phys.* **1994**, *186*, 435.

(7) Hanson, K.; Roskop, L.; Djurovich, P. I.; Zahariev, F.; Gordon, M. S.; Thompson, M. E. *J. Am. Chem. Soc.* **2010**, *132*, 16247.

(8) Siegl, W. O. *J. Org. Chem.* **1977**, *42*, 1872.

addition of alkyl or aryl amines to substituted 1,2-dicyanobenzene. The compounds were characterized by ^1H and ^{13}C NMR, high resolution mass spectrometry, and absorption and emission spectroscopy.

Table 1. Synthesis of **BPI** and Substituted 1,3-Bis(aryl- or alkylimino)isoindoline Dyes **1–7**



compound	R ₁	R ₂	R ₃	yield (%)
BPI	2-pyridyl	H	H	–
1	2-pyridyl	OH	H	24
2	2-pyridyl	OEt	H	12
3^a	2-pyridyl	OH, OEt	H	7
4^b	2-pyridyl	OH	Cl	18
5	<i>n</i> -C ₁₂ H ₂₅	OH	H	34
6^b	4- <i>t</i> -Bu-phenyl	OH	H	6
7^b	1-isoquinolyl	OH	H	15

^a Compound **3** was isolated as a side product during the preparation of **2**. ^b Prepared in refluxing *n*-hexanol.

Single crystals of **1** and **2** suitable for X-ray diffraction analysis were obtained from saturated CH₂Cl₂ solutions; the structures are shown in Figure 1. Both compounds have metric parameters that are similar to **BPI**.⁹ Deviations in bond lengths and angles are less than 0.03 Å and 4° in **1** and 0.01 Å and 0.5° in **2**. The most pronounced structural difference between the two species is the average N1···O separation, 2.914(2) Å in **1** and 2.943(1) Å in **2**. The shorter N1···O separation in **1** is presumably due to hydrogen bonding, absent in **2**, between the hydroxyl protons and the imine nitrogens. The electron density map of **1** suggests that the hydroxyl protons are more closely bound to oxygen than to nitrogen ($d_{\text{O-H}} = 1.00(3)$ Å, $d_{\text{N-H}} = 2.05(3)$ Å), indicating that the enol tautomer is favored in the solid state. A ^1H NMR spectrum of **1** in CDCl₃ displays a sharp resonance at δ 13.3 ppm for the isoindoline N–H proton,⁹ however, no signal for the hydroxy protons is observed, which indicates that these protons undergo a rapid exchange process in fluid solution.

The absorption spectrum of **BPI** displays a series of transitions in the near-UV with the lowest energy transition at 405 nm (Figure 2). Although nonemissive at room temperature, **BPI** does luminesce in frozen 2-methyltetrahydrofuran (2-MeTHF) at 77 K, displaying a vibronically structured emission with an excited-state lifetime ($\tau = 3.4$ ns) and Stokes shift (~ 410 cm⁻¹) typical for fluorescence from a π - π^* state (Figure 2). The dihydroxylated derivative **1** (R₂ = OH) has a similar absorption profile with an absorption onset that is slightly red-shifted ($\lambda_{\text{max}} = 430$ nm) from the parent molecule. However, compound

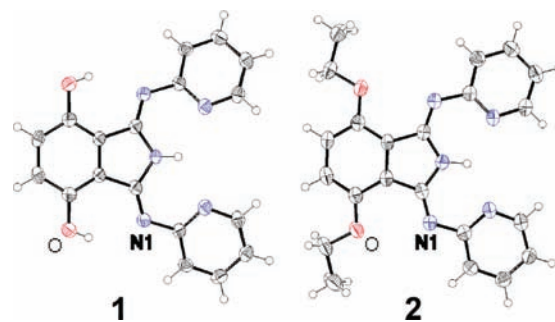


Figure 1. ORTEP drawings of compounds **1** and **2** (carbon (black), nitrogen (blue), oxygen (red), and hydrogen (white)).

1 is intensely emissive in CH₂Cl₂ at room temperature ($\Phi = 0.40$) and its luminescence spectrum displays a large apparent Stokes shift of 6600 cm⁻¹ ($\lambda_{\text{max}} = 597$ nm, Figure 2). The unusual emission characteristics prompted our further investigation into the photophysical properties of **1** and its derivatives.

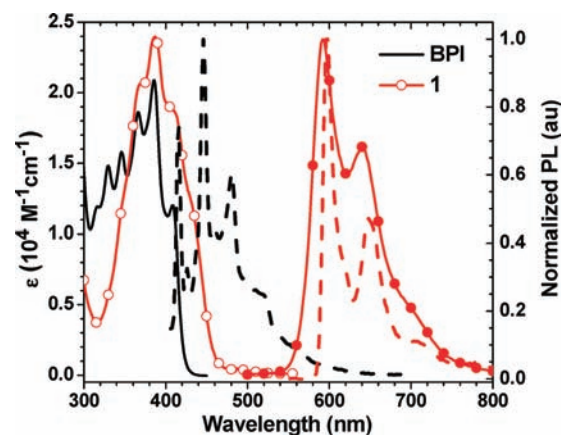


Figure 2. Absorption spectra of **BPI** (black) and **1** (red, empty circle) in CH₂Cl₂ at room temperature and emission spectra in 2-MeTHF at 77 K (dash) and in CH₂Cl₂ at room temperature (filled circle).

The absorption and emission spectra of **1** show minimal variation with solvent polarity, whereas the quantum efficiencies and excited-state lifetimes are significantly affected by different media (e.g., $\Phi = 0.28$, $\tau = 2.94$ ns in DMF; $\Phi = 0.45$, $\tau = 5.31$ ns in isopropanol). Upon cooling to 77 K in 2-MeTHF, the emission energy of **1** is little altered ($\lambda_{\text{max}} = 598$ nm) (Figure 2) although the excited-state lifetime does increase ($\tau_{\text{rt}} = 3.05$ ns, $\tau_{77\text{K}} = 5.11$ ns). The nanosecond lifetime, large apparent Stokes shift, and close proximity of a proton donor (hydroxyl) and acceptor (imine) are common characteristics of ES IPT dyes. The X-ray and ^1H NMR data for **1** argue that the enol tautomer is responsible for strong UV absorption transitions while emission originates from the keto tautomer. The vibronic structure displayed in the emission spectra

(9) Schilf, W. *J. Mol. Struct.* **2004**, *691*, 141.

indicates that the keto tautomer is a metastable bound state. The emission properties are retained in the presence of bases ($\text{Et}_3\text{N}/\text{CH}_2\text{Cl}_2$ or methanolic NaOH).

Table 2. Luminescent Properties of **BPI** and **1–7**

complex	solvent	emission at rt		
		λ_{max} (nm)	τ (ns)	Φ_{PL}^a
BPI	2-MeTHF	416 ^c	3.4	–
1	MeOH	592	3.7	0.31
	MeOD	593	6.7	0.69
	CH_2Cl_2	597	3.9	0.40
	Toluene	602	3.3	0.37
2	2-MeTHF ^b	452	3.7	–
3	MeOH	600	3.8	0.29
	MeOD	600	6.8	0.55
	CH_2Cl_2	615	4.6	0.39
	Toluene	622	4.1	0.34
4	MeOH	613	4.2	0.25
	CH_2Cl_2	612	4.6	0.39
	Toluene	614	3.6	0.35
5	MeOH	471, ^d 549 ^e	7.2, ^d 8.4 ^e	0.48
	CH_2Cl_2	469, ^d 567 ^e	6.8, ^d 7.9 ^e	0.06
	Toluene	575	7.3	0.05
6	MeOH	600	4.1	0.12
	CH_2Cl_2	604	3.7	0.02
	Toluene	590	3.1	0.04
7	MeOH	612	1.5 (4%), 4.0 (96%)	0.04
		CH_2Cl_2	612	1.0 (39%), 3.5 (41%)
	Toluene	620	1.0 (55%), 2.8 (45%)	0.04

^a Absolute quantum yield measured using an integrating sphere. ^b 77 K. ^c Highest energy peak. ^d Enol emission. ^e Keto emission.

Compound **2** ($\text{R}_2 = \text{OEt}$) was prepared since inhibition of proton transfer by alkylating the proton donor is a common means to verify the ESIPT process.¹⁰ The absorption and luminescent properties of **2** are similar to those of **BPI**: emission with a small Stokes shift ($\sim 1700 \text{ cm}^{-1}$) is only observed at 77 K (Figure 3). On the other hand, the photo-physical properties of the monoalkylated derivative **3** ($\text{R}_2 = \text{OH}$, OEt) are analogous to those of **1** (Figure 3, Table 2), which indicates that transfer of just a single hydroxyl proton is sufficient to enter the metastable luminescent state. Moreover, upon switching solvents from methanol to methanol-*d*₁, the quantum efficiencies of **1** and **3** increase 2-fold, from 0.31 to 0.69 for **1** and 0.29 to 0.55 for **3**. The large improvements in Φ are caused by a 4-fold decrease in the rate of nonradiative deactivation in **1** ($k_{\text{nr}(\text{MeOH})} = 1.9 \times 10^8 \text{ s}^{-1}$, $k_{\text{nr}(\text{MeOD})} = 4.6 \times 10^7 \text{ s}^{-1}$) and a 3-fold decrease in **3** ($k_{\text{nr}(\text{MeOH})} = 1.9 \times 10^8 \text{ s}^{-1}$, $k_{\text{nr}(\text{MeOD})} = 6.5 \times 10^7 \text{ s}^{-1}$). The pronounced effect of deuteration on the nonradiative rates indicates that N–H-(D) vibrations are associated with prominent deactivation modes in the keto excited state.

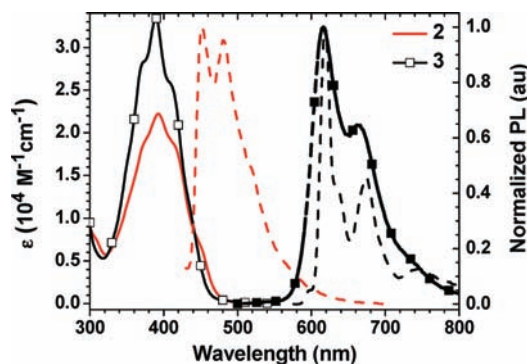


Figure 3. Absorption spectra of **2** (red) and **3** (black, empty square) in CH_2Cl_2 at room temperature and emission spectra in 2-MeTHF at 77 K (dash) and in CH_2Cl_2 at room temperature (filled square).

In contrast to compounds **1** and **3**, which show ground-state absorption primarily from the enol tautomer, compound **4** ($\text{R}_3 = \text{Cl}$) exhibits an equilibrium between absorbing species (enol or keto) that is strongly solvent dependent (Figure 4). In toluene, compound **4** displays an absorption profile similar to that of **1** ($\lambda_{\text{max}} = 400 \text{ nm}$, $\epsilon \approx 2.5 \times 10^4 \text{ M}^{-1} \text{ cm}^{-1}$). However, in CH_2Cl_2 , a vibronically structured, low-energy transition between 500 and 620 nm appears and becomes the primary absorption feature of **4** in methanol ($\lambda_{\text{max}} = 600 \text{ nm}$, $\epsilon \approx 2.8 \times 10^4 \text{ M}^{-1} \text{ cm}^{-1}$). The low-energy bands are assigned to transitions from the keto tautomer since they show a mirror-image relation with the emission spectra (Figure 4).

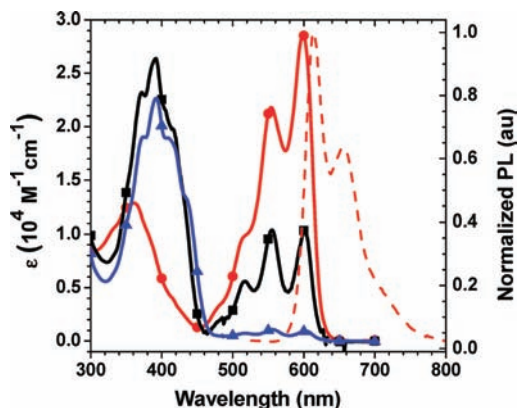


Figure 4. Absorption spectra of compound **4** in toluene (blue triangle), CH_2Cl_2 (black square), and MeOH (red circle) and the emission spectra in MeOH (dash) at room temperature.

The ESIPT behavior of **1**, **3**, and **4** is not surprising considering that dihydroxyphthalimide is also known to exhibit emission from an ESIPT state¹¹ and there is significant structural similarity between phthalimide and **BPI**. However, the 1,3-bis(imino)isoindole motif has two readily modifiable sites at R_1 (Table 1) that are not present in phthalimide. Therefore, compounds **5–7** were prepared

to examine the effects different imino substituents exert on the photophysical properties.

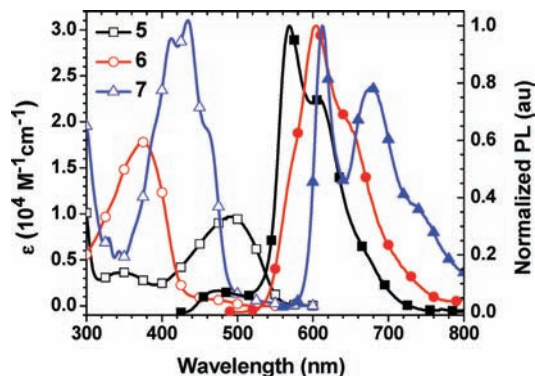


Figure 5. Absorption (empty shape) and emission (filled shape) spectra of compounds **5** (black, square), **6** (red, circle), and **7** (blue, triangle) in CH_2Cl_2 at room temperature.

The room-temperature absorption and emission spectra of **5–7** in CH_2Cl_2 are shown in Figure 5. Compound **5** ($R_1 = n\text{-C}_{12}\text{H}_{25}$) displays a band at low energy ($\lambda_{\text{max}} = 495 \text{ nm}$, $\epsilon \approx 1 \times 10^4 \text{ M}^{-1} \text{ cm}^{-1}$) that is assigned to the keto tautomer. The transition occurs at higher energy than that for the keto tautomers of **1**, **3**, and **4**, presumably due to the lack of conjugation with the imine nitrogen. The absorption profile of **6** ($R_1 = 4\text{-}t\text{-Bu-phenyl}$) is dominated by the higher energy, enol tautomer ($\lambda_{\text{max}} = 365 \text{ nm}$, $\epsilon \approx 1.8 \times 10^4 \text{ M}^{-1} \text{ cm}^{-1}$) in CH_2Cl_2 and toluene, whereas the keto tautomer is favored in methanol ($\lambda = 475\text{--}610 \text{ nm}$). The spectrum of the benzannulated derivative **7** ($R_1 = 1\text{-isoquinoyl}$) shows a red-shifted, enol transition ($\lambda = 350\text{--}500 \text{ nm}$, $\epsilon_{\text{max}} \approx 3 \times 10^4 \text{ M}^{-1} \text{ cm}^{-1}$) that does not vary significantly with solvent.

As shown in Figure 5, the emission from compound **5** is blue-shifted ($\lambda_{\text{em}} = 550\text{--}575 \text{ nm}$) relative to the other

derivatives. Upon excitation into the absorption band at 350 nm of **5**, a weak, high energy emission band is also observed near 470 nm in CH_2Cl_2 and methanol, likely due to fluorescence from the enol tautomer. The emission energy of compound **6** ($\lambda_{\text{em}} = 600\text{--}622 \text{ nm}$, Table 2) is similar to that of **1**, **3**, and **4** and varies little with solvent, although the quantum efficiency is much lower ($\Phi = 0.02\text{--}0.12$). Likewise, the emission energy of benzannulated compound **7** is minimally affected by solvent and the quantum efficiencies are significantly diminished ($\Phi = 0.03\text{--}0.04$). The emission lifetime cannot be fit to a single exponential, suggesting the presence of conformational isomers for the keto tautomer of **7**. Despite having lower quantum yields, the emission lifetimes for **5–7** are comparable to values for **1**, indicating that a significant fraction of nonradiative decay occurs prior to tautomerization to the luminescent species.

In summary, a new class of proton-transfer dyes based on the 1,3-bis(imino)isoindole diol motif has been introduced. The ESIPT nature of the luminescence was supported by inhibition of emission upon alkylation of the dihydroxylated **BPI**. Several derivatives of the parent ESIPT structure were prepared by nucleophilic addition of alkyl or aryl amines to substituted 1,2-dicyanobenzene. Modification of either the indole or imino substituents shifts the equilibrium between keto and enol forms of the molecule in both the ground and the excited state. The ability to alter the thermodynamics of proton transfer by such changes of the 1,3-bis(imino)isoindole can be used to investigate the structure–property relationships that control the excited-state proton transfer process with the long-term goal of developing guiding principles for ESIPT-luminophore design. A large variety of new ESIPT dyes can also be envisioned by tailoring the substituents around the 1,3-bis(imino)isoindole diol core.

Acknowledgment. The authors would like to thank Universal Display Corporation and the Department of Energy for their financial support of this work.

Supporting Information Available. Experimental procedures and full spectroscopic data for all compounds. This material is available free of charge via the Internet at <http://pubs.acs.org>.

(10) (a) Mordziński, A.; Grabowska, A. *Chem. Phys. Lett.* **1982**, *90*, 122. (b) Mordziński, A.; Grabowska, A.; Kühnle, W.; Kröwezyński, A. *Chem. Phys. Lett.* **1983**, *101*, 291. (c) Mutai, T.; Tomoda, H.; Ohkawa, T.; Yabe, Y.; Araki, K. *Angew. Chem., Int. Ed.* **2008**, *47*, 9522. (d) Sliwa, M.; Mouton, N.; Ruckebusch, C.; Poisson, L.; Idrissi, A.; Aloise, S.; Potier, L.; Dubois, J.; Poizat, O.; Buntinx, G. *Photochem. Photobiol. Sci.* **2010**, *9*, 661.

(11) (a) Gruzinskii, V. V.; Staneva, T. G. *Zhurnal Prikladnoi Spektroskopii* **1975**, *23*, 820. (b) Sultanova, N.; Staneva, T. *Proc. SPIE-Int. Soc. Opt. Eng.* **2003**, *5226*, 99. (c) Wakita, J.; Inoue, S.; Kawanishi, N.; Ando, S. *Macromolecules* **2010**, *43*, 3594.